

ORIGINAL ARTICLE

Synthesis and photovoltaic properties of low band gap copolymers containing (bithiophenevinyl)-(2-pyran-4-ylidenemalononitrile) (TVM) moieties

Weidong Cheng, Shiyu Yao, Shanpeng Wen, Pengfei Li, Hui Li, Lijuan Wang, Long Yan, Jinlong Chen, Jibo Zhang and Wenjing Tian

Three novel conjugated copolymers containing a coplanar bithiophenevinyl-(2-pyran-4-ylidenemalononitrile) unit linked with different electron-donating moieties by a double bond were synthesized via Heck polycondensation reactions and characterized using nuclear magnetic resonance, gel permeation chromatography and elemental analysis. Thermogravimetric analysis of the copolymers revealed that they have good thermal stability, with a decomposition temperature $> 330\text{ }^{\circ}\text{C}$. By eliminating torsional interactions between donor and acceptor units, combination by double bonds resulted in an enhancement of the conjugated length, extension of the absorption spectral range and a low band gap of the polymers. Cyclic voltammetry measurements suggest that the highest occupied molecular orbital and the lowest unoccupied molecular orbital energy levels of the copolymers can be fine-tuned by introducing donor units with different electron-donating ability. Bulk-heterojunction photovoltaic cells were fabricated with the copolymers as the donors and (6,6)-phenyl C_{71} -butyric acid methyl ester as the acceptor. The cells based on the three copolymers exhibited power-conversion efficiencies of 0.36, 0.41 and 0.47% under one sun of air mass 1.5 solar simulator illumination (100 mV cm^{-2}).

Polymer Journal (2013) 45, 1072–1080; doi:10.1038/pj.2013.36; published online 27 March 2013

Keywords: conjugated polymer; double bonds; photovoltaic devices; polymerization.

INTRODUCTION

Polymer solar cells (PSCs) have attracted significant attention due to their low cost, flexibility and large-area fabrication in comparison to inorganic solar cells^{1–7} and considerable progress has been made, as evidenced by the enhancement of the power-conversion efficiencies (PCEs) of PSCs from approximately 1% to $> 9\%$ over the past decade.⁸ PSCs usually adopt a bulk-heterojunction (BHJ) structure, where a phase-separated blend of donor and acceptor materials is used as the active layer.⁹ In most cases, fullerene derivatives, such as (6,6)-phenyl- C_{61} -butyric acid methyl ester (PC_{61}BM) or (6,6)-phenyl- C_{71} -butyric acid methyl ester (PC_{71}BM), are used as acceptors, and conjugated polymers are used as donors. Because most of the solar energy is harvested by donor polymers, extensive research efforts have been devoted to developing low band gap-conjugated polymers for PSCs.^{10–13} However, the open-circuit voltage (V_{oc}) of PSCs is closely related to the difference between the highest occupied molecular orbital (HOMO) energy level of the donor material and the lowest unoccupied molecular orbital (LUMO) energy level of the acceptor material (6,6-phenyl- C_{61} -butyric acid methyl ester PC_{61}BM). Therefore, both the HOMO energy level and the band gap of the

donor polymer are important factors in determining the PCEs of PSCs.¹⁴

Poly(3-hexylthiophene) (P3HT) is used as a typical donor material, and the PSC based on P3HT and PC_{61}BM has exhibited a high device efficiency of 5–6%.^{15,16} However, the narrow absorption spectrum of P3HT (300–650 nm) is one of the main hindrances to further enhancement of the efficiency. Therefore, enormous efforts have been devoted to developing low band gap-conjugated polymers^{17,18} due to their red-shifted and extended absorption in the visible region. Many studies demonstrate that incorporating alternating donor (D) and acceptor (A) moieties into the polymer main chain is an effective method to achieve low band gap polymers, as the intramolecular charge transfer (ICT) transition from donor to acceptor inside D-A copolymers can absorb photons with low energy (in long wavelength), which will extend the absorption spectral range and reduce the band gap of the polymer. In addition, the strength of ICT, the physical properties and even the energy level of the polymers can be tuned flexibly by changing the donor or acceptor units or the linking bridge between the donor and the acceptor.^{19,20} In this regard, many electron-rich units, such as 2,7-carbazole,²¹

indolo[3,2-*b*]carbazole,²² cyclopenta[2,1-*b*:3,4-*b'*]dithiophene,²³ dithieno[3,2-*b*:2,3-*d'*]silole,²⁴ and benzo-[1,2-*b*:4,5-*b'*]dithiophene,²⁵ and quite a few electron-deficient units, such as 2,1,3-benzothiadiazole,²⁶ diketopyrrolo[3,4-*c'*]pyrrole-1,4-dione,²⁷ ester- or ketone-substituted thieno[3,4-*b'*]thiophene,²⁸ and thieno[3,4-*c'*]pyrrole-4,6-dione,²⁹ have been developed; typically, they have been connected with each other through a single bond inside the polymer.

In our previous work, we synthesized a D-A polymer Poly{(10-hexyl-10H-phenothiazine-3,7-ylene)-alt-2-(2,6-bis((E)-2-(5-bromo-3,4-dihexylthiophen-2-yl) vinyl)-4H-pyran-4-ylidene)malononitril} (PPTMT) and fabricated a PSC using PPTMT as the donor and (6,6)-phenyl C₆₁-butyric acid methyl ester (PC₆₁BM) as the acceptor.³⁰ However, the ultraviolet (UV)-vis absorption edge of PPTMT was only located at 650 nm, which was not able to match the solar spectra well because of the relatively wide band gap (1.91 eV). Here, to further reduce the band gap for improved sunlight harvesting, we synthesized the copolymer P3 by incorporating a double bond instead of a single bond between the bithiophenevinyl-(2-pyran-4-ylidenemalononitrile) (TVM) unit and the phenothiazine unit. For comparison, polymers P1 and P2 were synthesized using a carbazole unit and a triphenylamine unit instead of a phenothiazine unit, which resulted in various degrees of ICT in the conjugated system to permit tuning of the band gap and HOMO/LUMO energy levels. The structures of PPTMT, P1, P2 and P3 are shown in Scheme 1.

The introduction of the double bond can improve the coplanar property of the polymers by hindering or restricting the rotation of the TVM unit and donor units to enhance the π - π stacking of the copolymer in the solid state.³¹ In addition, it can also extend the conjugated length of the copolymer to reduce the band gap and broaden the UV-vis absorption spectra. The three copolymers exhibited lower optical band gaps of 1.82, 1.79 and 1.71 eV. Compared with the similar PPTMT structure, the optical absorption of P3 in the film exhibited a broader and approximately 70 nm red-shifted absorption band with an absorption edge near 720 nm. Although the HOMO energy level of P3 was increased (-5.10 eV) compared with that of PPTMT (-5.25 eV), when the phenothiazine unit was replaced by a triphenylamine and carbazole unit, the HOMO energy level decreased to -5.14 eV and -5.17 eV, respectively. The PCEs of

the BHJ PSCs based on P1: PC₇₁BM, P2: PC₇₁BM and P3: PC₇₁BM reached 0.36, 0.41 and 0.47%, respectively, under one sun of air mass (AM) 1.5 solar simulator illumination (100 mV cm⁻²).

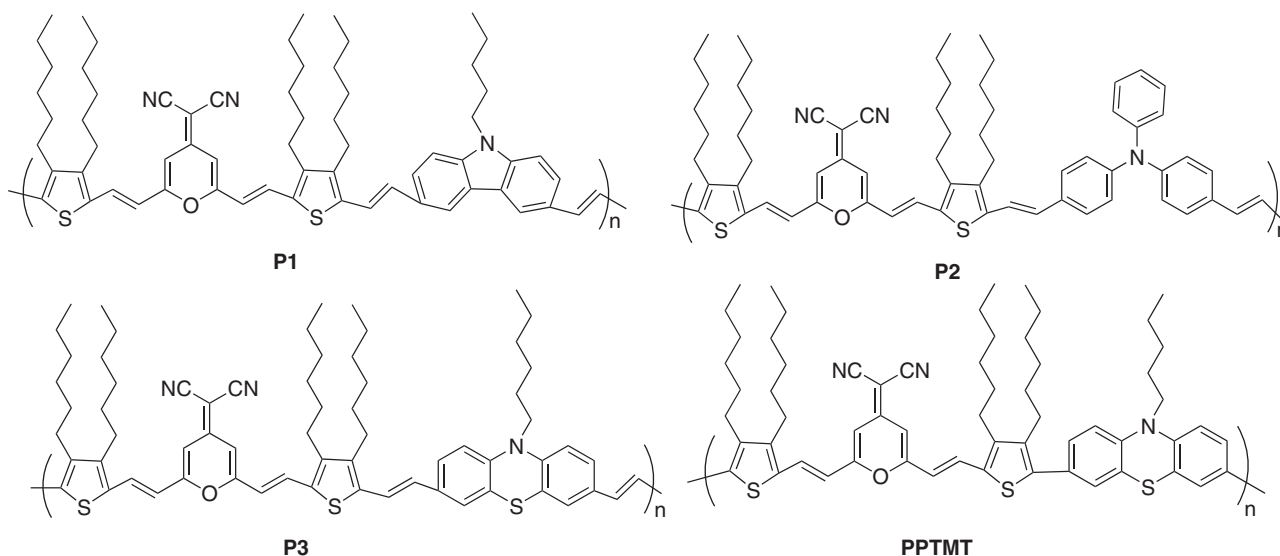
EXPERIMENTAL PROCEDURE

2.1. Characterization

The elemental analysis was performed using a Thermoquest CHNS-Ovelemental analyzer (Perkin-Elmer Corporation, Waltham, MA, USA). Gel permeation chromatographic analysis was performed using a Waters 410 instrument (Waters Technologies (Shanghai) Limited, Shanghai, China) with tetrahydrofuran (THF) as the eluent (flow rate: 1 ml min⁻¹, at 35 °C) and polystyrene as the standard. Thermal gravimetric analysis was performed on a Perkin-Elmer Pyris 1 analyzer (Perkin-Elmer) under a nitrogen atmosphere (100 ml min⁻¹) at a heating rate of 10 °C min⁻¹. ¹H nuclear magnetic resonance (NMR) and ¹³C NMR spectra were collected using a Bruker AVANCE-500 NMR spectrometer (Bruker Corporation, Billerica, MA, USA) and a Varian Mercury-300 NMR (Varian Corporation, Salt Lake City, UT, USA), respectively. UV-vis absorption spectra were collected using a Shimadzu UV-3100 spectrophotometer (Shimadzu Corporation, Tokyo, Japan). Electrochemical measurements of these derivatives were performed with a Bioanalytical Systems BAS 100 B/W electrochemical workstation (Bioanalytical Systems, Inc., West Lafayette, IN, USA). Atomic force microscopic images of the blend films were obtained using a NanoscopeIIa Dimension 3100 (Bruker Corporation, Billerica, MA, USA).

Photovoltaic device fabrication and characterization

The BHJ solar cells were fabricated with the active layer consisting of the copolymers PC₇₁BM with varied blend ratios. Indium tin oxide (ITO) glass was cleaned using alcohol, acetone and isopropyl alcohol and pretreated with ultraviolet ozone plasma for 10 min. A 40-nm layer of poly(3,4-ethylene dioxythiophene):poly(styrenesulfonate) (PEDOT:T: PSS) (Bayer PVP Al 4083, Bayer (Beijing) Sheet Company Ltd., Beijing, China), as a modified layer, was spin-coated onto the pre-cleaned ITO glass substrate and then dried at 120 °C for 15 min on a hot plate. The copolymers were dissolved in chlorobenzene to prepare 20 mg ml⁻¹ solutions, followed by blending with PC₇₁BM (purchased from Lumtec Corp., Hsinchu City, Taiwan, China) in varied blend ratios. The active layers were obtained by spin-coating the blend solutions, and the thicknesses of the films were approximately 50–70 nm, as measured with a Veeco DEKTAK 150 surface profilometer (Beijing Branch of Veeco Corporation, Beijing, China). Finally, a LiF (0.6 nm)/Al (100 nm) cathode was thermally deposited to complete the device fabrication. The active area was

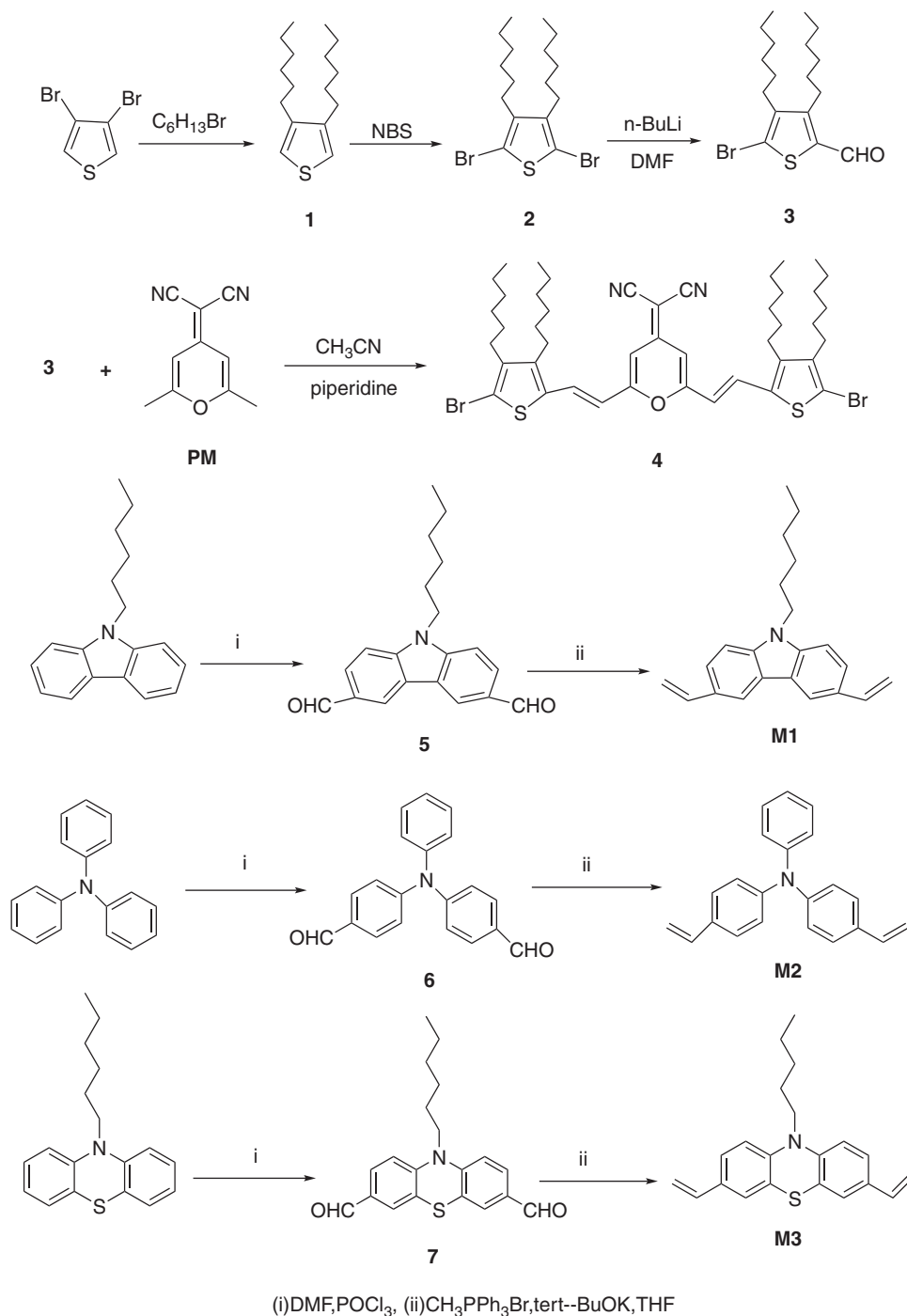


Scheme 1 The molecular structure of PPTMT (poly{(10-hexyl-10H-phenothiazine-3,7-ylene)-alt-2-(2,6-bis((E)-2-(5-bromo-3,4-dihexylthiophen-2-yl) vinyl)-4H-pyran-4-ylidene)malononitril}), P1, P2 and P3.

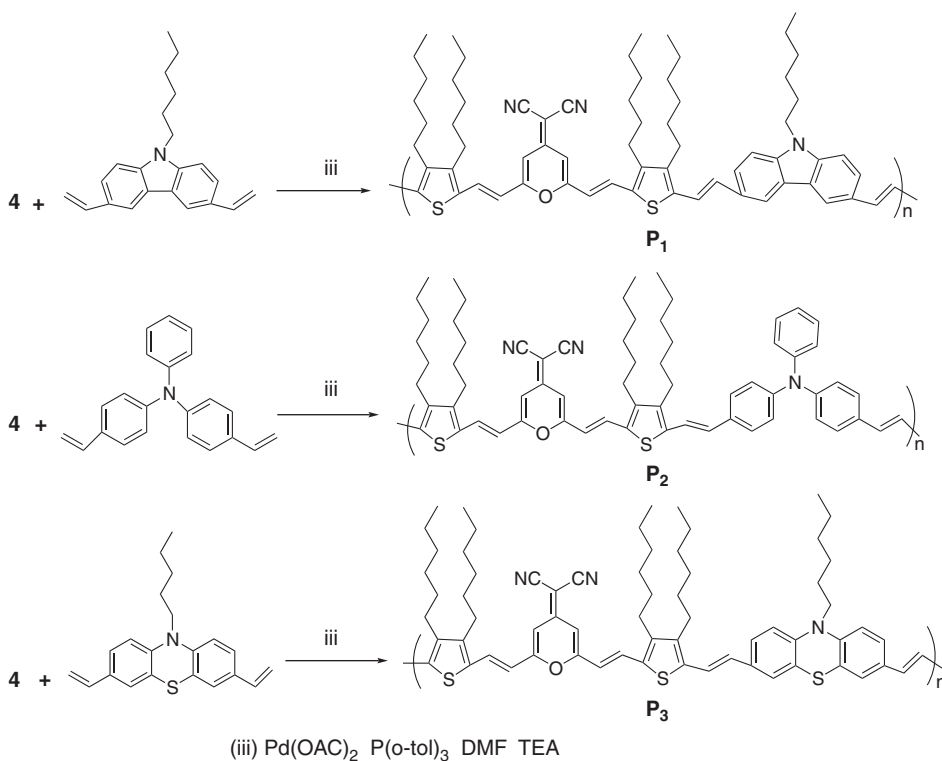
approximately 5 mm^2 . The current–voltage (J – V) characteristics were recorded using a Keithley 2400 Source Meter (Keithley Instruments, Inc., Beijing, China) in the dark and under 100 mW cm^{-2} simulated AM 1.5 illumination (100 mW cm^{-2}) by Solar Simulators (SCIENCETECH SS-0.5K, Worldwide Technology Co. Ltd., Shanghai, China). The spectral response was recorded using an SR830 lock-in amplifier (Formosa Technology Corporation, New Taipei City, Tainan, China) under short-circuit conditions, under which the devices were illuminated with a monochromatic light from a Xeon lamp. All fabrication and characterizations were performed in an ambient atmosphere at room temperature.

Materials

9-Heptyl-9H-carbazole, 10-hexylphenothiazine and 2-(2,6-dimethyl-4H-pyran-4-ylidene)malononitrile (PM) were synthesized according to the literature procedures.^{32–35} The compounds 1–4 were synthesized according to the literature procedures.³⁰ All other reagents and chemicals were purchased from commercial sources (Aldrich (Shanghai, China), Acros (Beijing, China), Fluka (Shanghai, China), Beijing Chemical Reagent (Beijing, China) and J&K (Shanghai, China)) and used without further purification unless stated otherwise. All of the solvents were distilled over an appropriate drying agent before use and were purged with nitrogen.



Scheme 2 Synthesis routes of the monomers.



Scheme 3 Synthesis routes of the copolymers P1, P2 and P3.

Synthesis

Synthesis of monomers. The synthetic routes of the monomers and polymers are illustrated in Schemes 2 and 3, respectively.

Synthesis of 9-hexyl-9H-carbazole-3,6-dicarbaldehyde (5). To DMF (30.78 ml, 397.8 mmol) and 9-heptyl-9H-carbazole (5.0 g 20 mmol), cooled to 0 °C with an ice salt bath, phosphorus oxychloride (34.7 ml, 397.8 mmol) was added dropwise with stirring for an hour; the stirred yellow solution was allowed to heat to 100 °C. After 24 h, the black solution was slowly poured into ice water and then extracted with dichloromethane. The organic layer was washed with water and dried over anhydrous magnesium sulfate. After the removal of solvents, the crude product was purified via column chromatography (petroleum-ether/dichloromethane 4: 3, v/v) and dried under vacuum to yield a light yellow solid (2.1 g, 34%). ¹H NMR (300 MHz, CDCl₃, tetramethylsilane (TMS)): δ (p.p.m.) 10.14 (s, 2H, -CHO), 8.68 (d, 2H, J = 0.9 Hz, -Ar), 8.11 (d, 1H, J = 1.5 Hz), 8.08 (d, 1H, J = 1.5 Hz), 7.57 (s, 1H), 7.54 (s, 1H), 4.39 (t, 2H, J = 7.2 Hz, -αCH₂), 1.92 (m, 2H, -CH₂), 1.54-1.27 (m, 6H, -CH₂), 0.86 (m, 3H, -CH₃). Elem. Anal. Calcd. for: C₂₀H₂₁NO₂: C, 78.13; H, 6.89. Found: C, 78.20; H, 6.79. High resolution mass spectrometer (HRMS) (*m/z*, EI⁺) calcd for C₂₀H₂₁NO₂: 307.1654, found 307.1656.

Synthesis of 4,4'-(phenylazanediy)l)dibenzaldehyde (6). The synthesis process was similar to that of (5) to yield a light yellow solid with a yield of 50%. ¹H NMR (300 MHz, CDCl₃, TMS): δ (p.p.m.) 9.89 (s, 2H, -CHO), 7.79 (t, 2H, J = 2.1 Hz), 7.76 (t, 2H, J = 2.1 Hz), 7.42-7.37 (m, 2H), 7.28-7.16 (m, 7H). Elem. Anal. Calcd. for C₂₀H₁₅NO₂: C, 79.78; H, 4.92. Found: C, 79.75; H, 5.00. HRMS (*m/z*, EI⁺) calcd for C₂₀H₁₅NO₂: 301.1192, found 301.1195.

Synthesis of 10-hexyl-10H-phenothiazine-3,7-dicarbaldehyde (7). The synthesis process was similar to that of (5) to yield an orange solid with a yield of 45%. ¹H NMR (300 MHz, CDCl₃, TMS): δ (p.p.m.) 9.82 (s, 2H, -CHO), 7.68 (d, 1H, J = 1.8 Hz, -Ar), 7.65 (d, 1H, J = 2.1 Hz, -Ar), 7.59 (d, 1H, J = 1.8 Hz, -Ar), 6.97 (s, 1H, -Ar), 6.94 (s, 1H, -Ar), 3.94 (t, 2H, J = 7.2 Hz, -αCH₂), 1.81 (m, 2H, -CH₂), 1.46 (m, 2H, -CH₂), 1.35-1.29 (m, 4H, -CH₂), 0.88 (m, 3H, -

CH₃). Elem. Anal. Calcd. for C₂₀H₂₁NO₂S: C, 70.79; H, 6.26; Found: C, 70.80; H, 6.27. HRMS (*m/z*, EI⁺) calcd for C₂₀H₂₁NO₂S: 339.1320, found 339.1322.

Synthesis of 9-hexyl-3,6-divinyl-9H-carbazole (M1). A mixture of methyl-triphenylphosphonium bromide (5.23 g, 14.6 mmol) and potassium tert-butoxide (1.91 g, 17.0 mmol) and THF (50 ml) was stirred for 10 min under N₂. A solution of compound 5 (1.5 g, 4.88 mol) and THF (10 ml) was injected by syringe and stirred for 24 h at room temperature. The yellow mixture was subsequently slowly poured into water and extracted with dichloromethane. Then, the organic layer was dried with anhydrous magnesium sulfate. After removal of the solvents, the remaining yellow-green liquid was purified via column chromatography (petroleum ether/dichloromethane 9: 1 v/v) and dried under vacuum to yield M1 as a yellow-green viscous oil, 0.44 g (1.46 mmol, yield 30%). ¹H NMR (300 MHz, CDCl₃, TMS): δ (p.p.m.) 8.12 (s, 2H, -Ar), 7.57 (d, 2H, J = 8.4 Hz, -Ar), 7.33 (d, 2H, J = 8.4 Hz, -Ar), 6.91 (q, 2H, -vinyl), 5.78 (d, 2H, J = 17.7 Hz, -vinyl), 5.20 (d, 2H, J = 10.8 Hz, -vinyl), 4.26 (t, 2H, -αCH₂), 2.26 (m, 2H, -CH₂), 1.60 (m, 2H, -CH₂), 1.25 (m, 4H, -CH₂), 0.86 (t, 3H, -CH₃). ¹³C NMR (75 MHz, CDCl₃, TMS): δ (p.p.m.) 140.65, 137.45, 128.97, 124.08, 123.05, 118.41, 111.01, 108.77, 43.23, 31.54, 28.94, 26.90, 22.50, 13.98. Elem. Anal. Calcd. for: C₂₂H₂₅N: C, 87.09; H, 8.32. Found: C, 87.10; H, 8.27. HRMS (*m/z*, EI⁺) calcd for C₂₂H₂₅N: 303.2078, found 303.2080.

Synthesis of N-phenyl-4-vinyl-N-(4-vinylphenyl)aniline (M2). The synthesis process was similar to that of (M1) to yield a yellow-green viscous oil with a yield of 72%. ¹H NMR (300 MHz, CDCl₃, TMS): δ (p.p.m.) 7.28-7.20 (m, 6H, -Ar), 7.10-7.00 (m, 7H, -Ar), 6.64 (q, 2H, -vinyl) 5.62 (d, 2H, J = 17.4 Hz, -vinyl), 5.14 (d, 2H, J = 11.1 Hz, -vinyl). ¹³C NMR (75 MHz, CDCl₃, TMS): δ (p.p.m.) 147.32, 147.17, 136.14, 132.08, 129.26, 127.05, 124.51, 123.80, 123.11, 112.25. Elem. Anal. Calcd. for: C₂₂H₁₉N: C, 88.87; H, 6.48. Found: C, 88.79; H, 6.40. HRMS (*m/z*, EI⁺) calcd for C₂₂H₁₉N: 297.1562, found 297.1560.

Synthesis of 10-hexyl-3,7-divinyl-10H-phenothiazine (M3). The synthesis process was similar to that of (M1) to yield a yellow-green viscous oil with a yield of 45%. ¹H NMR (300 MHz, CDCl₃, TMS): δ (p.p.m.) 7.17 (s, 2H),

7.14 (d, 2H, $J = 2.1$ Hz), 6.77 (d, 2H, $J = 8.1$ Hz), 6.58 (q, 2H, -vinyl), 5.60 (d, 2H, $J = 17.7$ Hz, -CH₂), 5.13 (d, 2H, $J = 10.8$ Hz, -CH₂), 3.81 (t, 2H, - α CH₂), 1.78 (m, 2H, -CH₂), 1.41 (m, 2H, -CH₂), 1.31-1.25 (m, 4H, -CH₂), 0.87 (t, 3H, -CH₃). ¹³C NMR (75 MHz, CDCl₃, TMS): δ (p.p.m.) 144.33, 135.45, 132.06, 125.36, 124.73, 124.27, 114.98, 112.05, 47.48, 31.39, 26.69, 26.53, 22.55, 13.95. Elem. Anal. Calcd. for C₂₂H₂₅NS: C, 78.78; H, 7.55. Found: C, 78.70; H, 7.6. HRMS (m/z , EI⁺) calcd for C₂₂H₂₅NS: 335.1726, found 335.1728.

Polymerization. All of the polymerization reactions and manipulations were performed under a nitrogen atmosphere. The preparation of P1, P2 and P3 was conducted using the modified Heck method, as illustrated in Scheme 3.

A flask was charged with a mixture of 2-(2,6-bis((E)-2-(5-bromo-3,4-dihexylthiophen-2-yl)vinyl)-4H-pyran-4-ylidene)-malononitrile (**4**), 9-hexyl-3,6-divinyl-9H-carbazole (**M1**), N-phenyl-4-vinyl-N-(4-vinylphenyl) aniline (**M2**), 10-hexyl-3,7-divinyl-10H-phenothiazine (**M3**), Pd(OAc)₂ (5 mol% with respect to the monomer), P(*o*-tolyl)₃ (20 mol%) and DMF (6 ml), and the mixture was stirred at room temperature for 30 min. After adding triethylamine (2 ml), the flask was degassed and purged with N₂. The mixture was heated at 100 °C for 48 h under N₂. The mixture was then filtered, and the filtrate was poured into methanol. The dark red precipitated solid was extracted with methanol for 24 h in a Soxhlet apparatus to remove the oligomers and catalyst residues. The soluble fraction was then collected via extraction with CHCl₃ for 24 h. The chloroform solution was then concentrated to produce the copolymers.

Synthesis of poly2-(2-((E)-2-(3,4-dihexyl-5-((E)-2-(9-hexyl-6-vinyl-9H-carbazol-3-yl)vinyl)thiophen-2-yl)vinyl)-6-((E)-2-(3,4-dihexylthiophen-2-yl)vinyl)-4H-pyran-4-ylidene)malononitrile (P1). The resulting polymer was a dark brittle solid with a yield of 35%. ¹H NMR (500 MHz, CDCl₃, TMS): δ (p.p.m.) 8.26-8.21 (m, 2H, -Ph), 7.66-7.62 (m, 2H, -vinyl), 7.42-7.37 (m, 2H, -Ph), 7.04 (s, 2H, -Ph), 6.61 (s, 2H, -PM), 6.53-6.46 (m, 2H, -vinyl), 5.80 (d, 2H, -vinyl), 5.23 (d, 2H, -vinyl), 4.31 (t, 2H, - α CH₂), 2.71 (t, 4H, -CH₂), 2.52 (t, 4H, -CH₂), 1.38-1.31 (m, 40H, -CH₂), 0.92-0.85 (m, 15H, -CH₃). Elem. Anal. Calcd. for C₆₆H₈₁N₃OS₂: C, 79.39; H, 8.38. Found: C, 78.48; H, 9.27.

Synthesis of poly2-(2-((E)-2-(3,4-dihexyl-5-(4-(phenyl(4-vinylphenyl)amino)styryl)thiophen-2-yl)vinyl)-6-((E)-2-(3,4-dihexylthiophen-2-yl)vinyl)-4H-pyran-4-ylidene)malononitrile (P2). The resulting polymer was a dark brittle solid with a yield of 42%. ¹H NMR (500 MHz, CDCl₃, TMS): δ (p.p.m.) 7.62-7.60 (m, 2H, -vinyl), 7.40-7.26 (m, 9H, -Ph), 7.14-7.03 (m, 4H, -Ph), 6.60 (s, 2H, -PM), 6.51-6.44 (m, 2H, -vinyl), 5.67 (d, 2H, -vinyl), 5.19 (d, 2H, -vinyl), 2.71-2.51 (m, 8H, - α CH₂), 1.42-1.26 (m, 32H, -CH₂), 0.91-0.84 (m, 12H, -CH₃). Elem. Anal. Calcd. for C₆₆H₇₅N₃OS₂: C, 79.87; H, 7.82. Found: C, 80.69; H, 7.01.

Synthesis of poly2-(2-((E)-2-(3,4-dihexyl-5-((E)-2-(10-hexyl-7-((E)-prop-1-enyl-10H-phenothiazin-3-yl)vinyl)thiophen-2-yl)vinyl)-6-((E)-2-(3,4-dihexyl-5-methylthiophen-2-yl)vinyl)-4H-pyran-4-ylidene)malononitrile (P3). The resulting polymer was dark brittle solid with a yield of 36%. ¹H NMR (500 MHz, CDCl₃, TMS): δ (p.p.m.) 7.64-7.59 (m, 2H, -vinyl), 7.19-7.17 (m, 2H, -Ar), 7.11-7.07 (m, 2H, -Ar), 6.88-6.81 (m, 2H, -Ar), 6.60 (s, 2H, -PM), 6.51-6.43 (m, 2H, -vinyl), 5.32 (d, 2H, -vinyl), 5.15 (d, 2H, -vinyl), 3.85 (t, 2H, -N- α CH₂), 2.68 (t, 4H, - α CH₂), 2.63 (t, 4H, - α CH₂), 1.54-1.26 (m, 40H, -CH₂), 0.93-0.84 (m, 15H, -CH₃). Elem. Anal. Calcd. for C₆₆H₈₁N₃OS₂: C, 76.92; H, 8.12. Found: C, 77.88; H, 7.62.

RESULTS AND DISCUSSION

Synthesis and characterization

The general synthetic strategy for the monomers and polymers is presented in Schemes 2 and 3. 2-(2,6-Bis((E)-2-(5-bromo-3,4-dihexylthiophen-2-yl)vinyl)-4H-pyran-4-ylidene)-malononitrile (**4**) was synthesized via the Knoevenagel reaction. To increase the solubility of **M1** and **M3**, a flexible brominated hexane was added to produce 9-heptyl-9H-carbazole and 10-hexylphenothiazine, which were converted to correspondent **5** and **7** via the well-known Vilsmeier reaction and then to 9-hexyl-3,6-divinyl-9H-carbazole

(**M1**) and 10-hexyl-3,7-divinyl-10H-phenothiazine (**M3**). N-phenyl-4-vinyl-N-(4-vinylphenyl)aniline (**M2**) was synthesized with commercially available triphenylamine as the starting material. In the Vilsmeier reaction, excessive quantity of DMF should be added; otherwise, mostly monoformylarylamine will be obtained. In addition, in the conversion from aldehyde to vinylene, we added potassium tert-butoxide as a strong base under the heating condition instead of *n*-BuLi at -40 °C,²⁴ which can attain higher yields. Because styrene is less stable and radical polymerization occurs at room temperature under irradiation, **M1**, **M2**, and **M3** should be copolymerized rapidly with **4** via the Heck coupling reaction with Pd(OAc)₂ and P(*o*-tolyl)₃ as the catalysts and triethylamine as a base in DMF to obtain the copolymers. The synthesized copolymers were highly soluble in common organic solvents such as chloroform, THF and chlorobenzene at room temperature.

Molecular weights and thermal properties

The molecular weights of the resulting copolymers are listed in Table 1. Using THF as the eluent and polystyrene as the standard, the gel permeation chromatographic data indicate a number-average (M_n) molecular weight from 16 400–43 700 and a weight-average (M_w) molecular weight from 4220–11 700. The polydispersity index ranges from 3.58 to 4.3.

Figure 1 presents the thermal gravimetric analysis (TGA) curves of the synthesized copolymers at the heating rate of 10 °C min⁻¹ under a nitrogen atmosphere. Compared with PPTMT (384 °C),³⁰ double bonds were introduced in the polymers, which can cause a decrease of the 5% weight-loss temperature (Td); however, the polymers also exhibit high thermal stability at 324, 346 and 341 °C. In addition, the high thermal stability of the resulting polymers prevents the deformation of the polymer morphology and degradation of the active layer in the PSCs.

Table 1 Polymerization results and thermal properties of copolymers

Polymers	M _w (kg mol ⁻¹)	M _n (kg mol ⁻¹)	PDI	TGA (T _d)
P1	4.22	18.1	4.30	324
P2	4.57	16.4	3.58	346
P3	11.7	43.7	3.70	341

Abbreviations: PDI, polydispersity index; TGA, thermal gravimetric analysis.

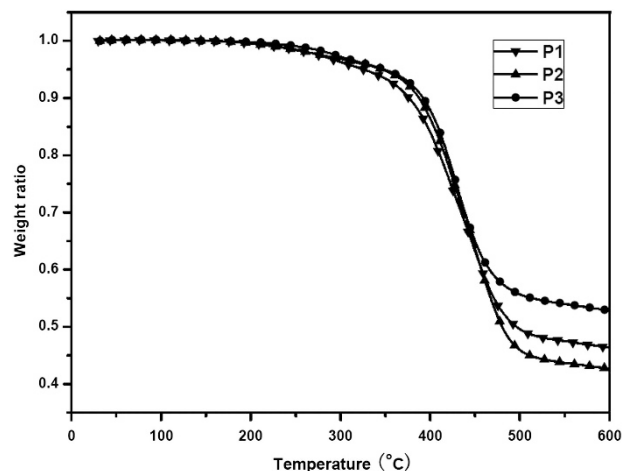


Figure 1 Thermal gravimetric analysis curves of copolymers at a heating rate of 10 °C min⁻¹ under a N₂ atmosphere.

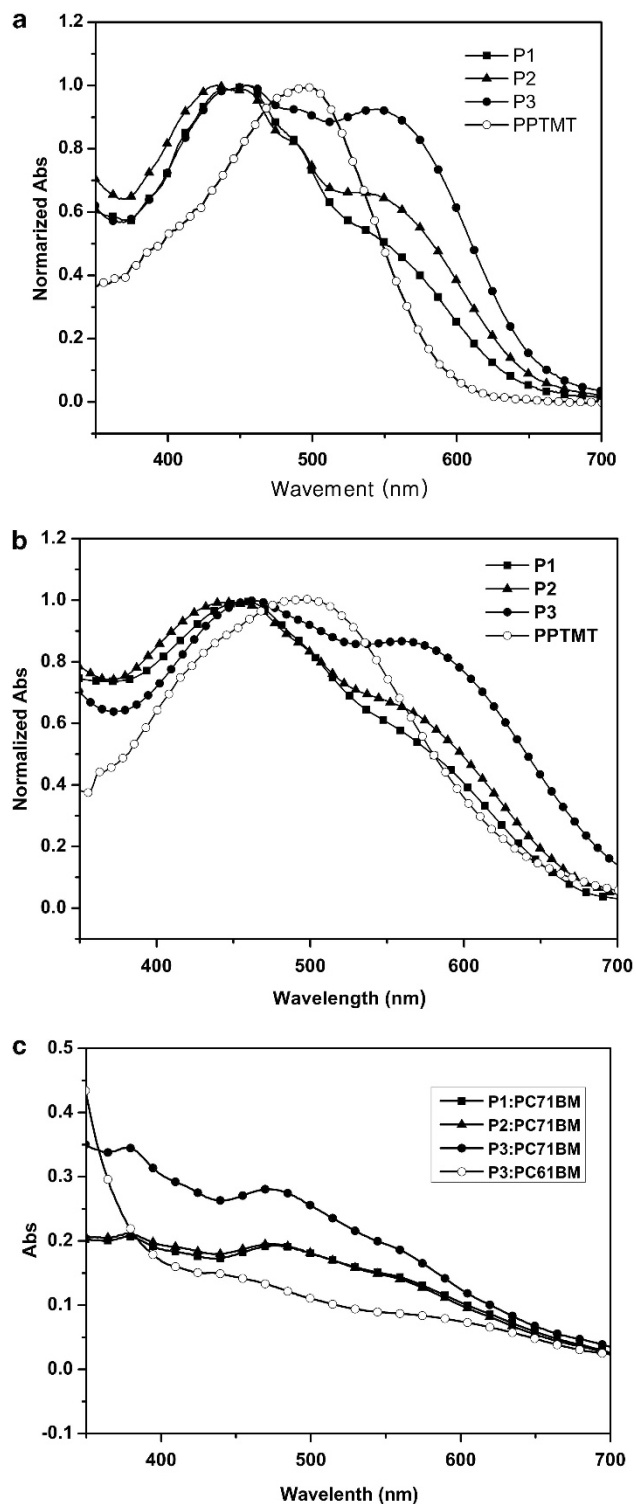


Figure 2 (a) Normalized absorption spectra of the copolymers in chloroform solutions with a concentration of $10^{-5} \text{ mol l}^{-1}$. (b) Normalized absorption spectra of the copolymer films spin-coated from a 5-mg ml^{-1} chlorobenzene solution. (c) The ultraviolet–vis spectra of the polymer/PC₇₁BM blend films. PPTMT, poly((10-hexyl-10H-phenothiazine-3,7-ylene)-alt-2-(2,6-bis((E)-2-(5-bromo-3,4-dihexylthiophen-2-yl) vinyl)-4H-pyran-4-ylidene)malononitri).

Table 2 Optical and electrochemical properties of copolymers

Polymers	$\lambda_{\text{max}}^{\text{abs, sol}}$ (nm)	$\lambda_{\text{max}}^{\text{abs, film}}$ (nm)	$E_{\text{g}}^{\text{opt}}$ (eV)	$E_{\text{onset}}^{\text{ox}}$ (V)	HOMO (eV)	$E_{\text{onset}}^{\text{red}}$ (V)	LUMO (eV)	E_{g}^{ec} (eV)
P1	456	465	1.82	0.42	-5.17	-1.22	-3.53	1.64
P2	434	444	1.79	0.39	-5.14	-1.26	-3.49	1.65
P3	456/550	466/564	1.71	0.35	-5.10	-1.30	-3.45	1.65
PPTMT	494	494	1.91	0.53	-5.25	-1.16	-3.56	1.69

Abbreviations: HOMO, highest occupied molecular orbital; LUMO, lowest unoccupied molecular orbital; PPTMT, poly((10-hexyl-10H-phenothiazine-3,7-ylene)-alt-2-(2,6-bis((E)-2-(5-bromo-3,4-dihexylthiophen-2-yl) vinyl)-4H-pyran-4-ylidene)malononitri).

Photophysical properties

The normalized UV–vis absorption spectra of P1, P2, P3 and PPTMT in dilute chloroform solution (concentration 10^{-5} M) are presented in Figure 2a, and the main optical properties are listed in Table 2.

In Figure 2a, the three new copolymers yield similar absorption spectra. P1, with a weak electron-donating carbazole unit, mainly exhibits one absorption band at 456 nm with a shoulder at approximately 530 nm in dilute solution, which can be assigned to the absorption of the π - π^* transition of the conjugated polymer backbone and the ICT interaction between the carbazole donor and the TVM-based acceptor.³⁶ In addition, the absorption spectra of the other copolymers (P2 and P3) in dilute solutions exhibited two bands at 434, 543 nm and 456, 550 nm due to the absorption of the π - π^* transition and the ICT interaction, which was red-shifted by 56 nm compared with PPTMT. Due to the three-dimensional structure of triphenylamine, the π - π^* transition is blue-shifted by 12 nm compared with P1 and P3. By contrast, the solution absorption spectrum of P3 is broadened and red-shifted compared with that of P1 and P2, which can be explained by the stronger ICT effect in P3.

The optical absorption spectra of the copolymers in the thin films (Figure 2b) are generally similar in shape to those in dilute solution. The absorption spectra also exhibit three peaks, with the maximum absorption peaks located at 465, 444 and 466 nm. Compared with their counterparts in dilute solution, the optical absorption of the polymers in the film were red-shifted by approximately 10 nm, presumably indicating the formation of a π -stacked structure in the solid state.^{37,38} From the optical edge of the absorption spectrum of the individual copolymer, the band gap of P1 was estimated to be 1.82 eV ($\lambda_{\text{edge}} = 681 \text{ nm}$), while lower band gaps of 1.79 and 1.71 eV were calculated for P2 and P3 ($\lambda_{\text{edge}} = 692$ and 720 nm), respectively. In comparison to the similar copolymer PPTMT ($\lambda_{\text{edge}} = 650 \text{ nm}$, $E_{\text{g}}^{\text{opt}} = 1.91 \text{ eV}$), the absorption spectra of P3 exhibited a broader and approximately 70 nm red-shifted absorption band, which indicated higher planarity along the polymer backbone due to the introduction of the double bonds. The UV–vis spectra of the polymer/PC₇₁BM blend films are also presented in Figure 2c. The spectra exhibit a broad absorption from 350 nm to approximately 650 nm. The film of P1:PC₇₁BM exhibited better absorption than the other films, and the result was also improved by external quantum efficiency (Figure 6).

Electrochemical properties

Cyclic voltammetry of the copolymer films was performed in acetonitrile with 0.1 M tetrabutylammonium-hexafluorophosphate (TBAPF₆) as the supporting electrolyte at a scan rate of 0.05 V s^{-1} with platinum button working electrodes, a platinum wire counter electrode and an Ag/AgNO₃ reference electrode under N₂ atmosphere. Ferrocene/ferrocenium (Fc/Fc⁺) was used as the internal standard.

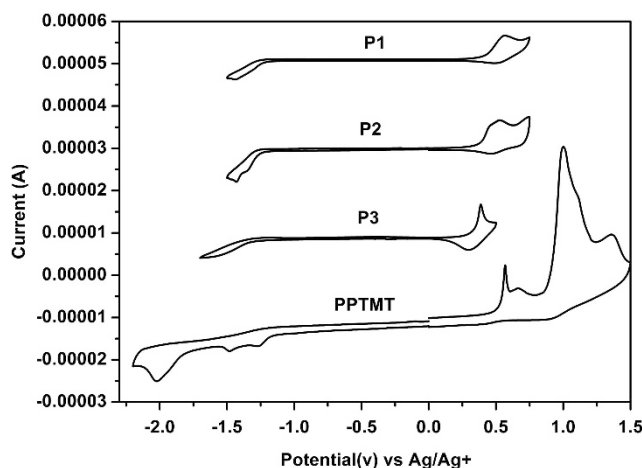


Figure 3 Cyclic voltammetry of copolymer thin films on Pt wires in 0.1 M tetrabutylammonium-hexafluorophosphate in acetonitrile. The scan rates used were 0.05 V s⁻¹.

The redox curves of the three polymers are presented in Figure 3 for comparison. On the anodic sweep, the three copolymers underwent a reversible oxidation with onset potentials of 0.42, 0.39 and 0.35 eV (versus Ag/Ag⁺). By contrast, the cathodic sweep resulted in onset reduction potentials from -1.22, -1.26 and -1.30 eV. The redox potential of Fc/Fc⁺, which has an absolute energy level of -4.8 eV relative to the vacuum level for calibration, is located at 0.05 V in the 0.1 M TBAPF₆/acetonitrile solution.³⁹ Therefore, evaluation of the HOMO and LUMO levels and the band gap (E_g^{ec}) could be performed according to the following equations:

$$\text{HOMO (eV)} = -e(E_{\text{ox}}^{\text{onset}} + 4.75) \text{ (eV)}$$

$$\text{LUMO (eV)} = -e(E_{\text{red}}^{\text{onset}} + 4.75) \text{ (eV)}$$

$$E_g^{ec} = E_{\text{ox}}^{\text{onset}} - E_{\text{red}}^{\text{onset}} \text{ (eV)}$$

where $E_{\text{ox}}^{\text{onset}}$ and $E_{\text{red}}^{\text{onset}}$ are the measured onset potentials relative to Ag/Ag⁺.

The results of the electrochemical measurements and the calculated energy levels of the copolymers are listed in Table 2. The HOMO energy level of donor polymers in a heterojunction photovoltaic cell is very important for high device efficiency because the V_{oc} of PSCs is related to the difference between the HOMO level of the donor polymer and the LUMO level of the acceptor. The relatively low HOMO level of the three new copolymers compared with that of polythiophene derivatives (for P3HT, HOMO = -4.75 eV)^{5,40} may be favored for the improvement of V_{oc} when fabricating PSCs with one of these polymers as the donor and PC₇₁BM as the acceptor. However, the energy offset between the LUMO energy levels of the polymer and PC₇₁BM (-3.9 eV) should be well controlled to be just large enough, and at least 0.3 eV, to provide a driving force for efficient charge separation.⁴ Here, the LUMO levels of the three copolymers are -3.53, -3.49 and -3.45 eV. In addition, the band gaps (E_g^{ec}) of the three copolymers were estimated to be approximately 1.65 eV. Therefore, the three copolymers have a low-lying LUMO level and a narrow band gap; accordingly, a high J_{sc} for the solar cells is expected. However, compared with PPTMT (-5.25), the HOMO level was obviously increased by introducing the double bands, which was unfavorable for the V_{oc} .

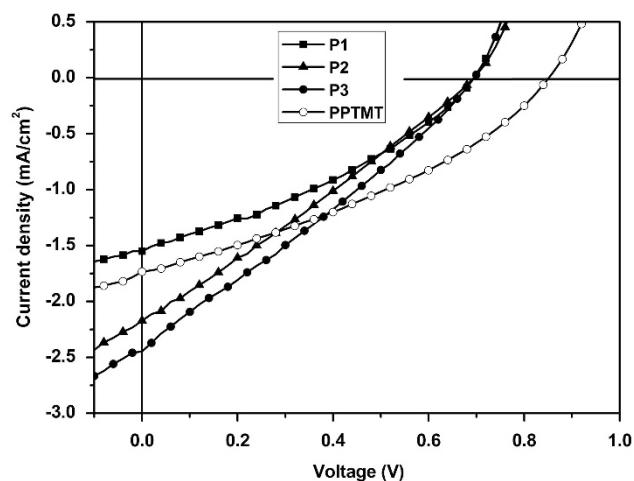


Figure 4 I-V curves of the polymer solar cells based on polymers/PC₇₁BM under AM 1.5, 100 mW cm⁻² illumination.

Table 3 Photovoltaic properties of the solar cells based on P:PC₇₁BM

P:PC ₇₁ BM	V_{oc} (V)	J_{sc} (mA cm ⁻²)	FF (%)	PCE (%)
P1(1:5)	0.69	1.55	33	0.36
P2(1:4)	0.69	2.17	27	0.41
P3(1:4)	0.69	2.44	28	0.47
PPTMT(1:3) ^a	0.86	1.73	34	0.51

Abbreviations: FF, fill factor; J_{sc} , short-circuit current; PCE, power-conversion efficiency; PPTMT, poly((10-hexyl-10H-phenothiazine-3,7-ylene)-alt-2-(2,6-bis((E)-2-(5-bromo-3,4-dihexylthiophen-2-yl) vinyl)-4H-pyran-4-ylidene)malononitril); V_{oc} , open-circuit voltage.
^aPhotovoltaic properties of PPTMT/PC₆₁BM-based devices spin-coated from a chlorobenzene solution for PPTMT.

Photovoltaic properties

To investigate the photovoltaic properties of the copolymers, BHJ PSCs with a structure of ITO/PEDOT: PSS/polymers: PC₇₁BM/LiF/Al were fabricated, where the copolymers were used as donors and PC₇₁BM was used as the acceptor. The solvents used for preparation of the active layer have a strong effect on the performance of PSCs.⁴¹ Here, we selected chlorobenzene as the solvent to obtain films of relatively good quality. Figure 4 presents the I-V curves of the devices, and Table 3 lists the corresponding V_{oc} , short-circuit current (J_{sc}), fill factor and PCE of the devices under AM 1.5, 100 mW cm⁻² illumination.

The V_{oc} of the PSCs is 0.69 V (by decreasing the voltage by 0.17 V with respect to PPTMT (0.86 V)) because the V_{oc} is related to the energy difference between the LUMO of the acceptor (PCBM) and the HOMO of the donor (conjugated polymer), as well as the morphology.^{42,43} Although the HOMO levels of the three copolymers are slightly different, the morphology is another influencing factor, which will be discussed below. The J_{sc} of P1, P2 and P3 increased, in order, to 1.55 mA cm⁻² for P1, to 2.17 mA cm⁻² for P2 and to 2.44 mA cm⁻² for P3. The PCEs of the PSCs based on P1, P2 and P3 were 0.36, 0.41 and 0.47%, respectively. The higher J_{sc} and PCE values of the devices based on P3 compared with the devices based on P1 and P2 may be attributed to the broader absorption and the lower band gap.

The film morphology of the blend film of the donor polymer and the acceptor (for example, PC₇₁BM) has been observed to be one of

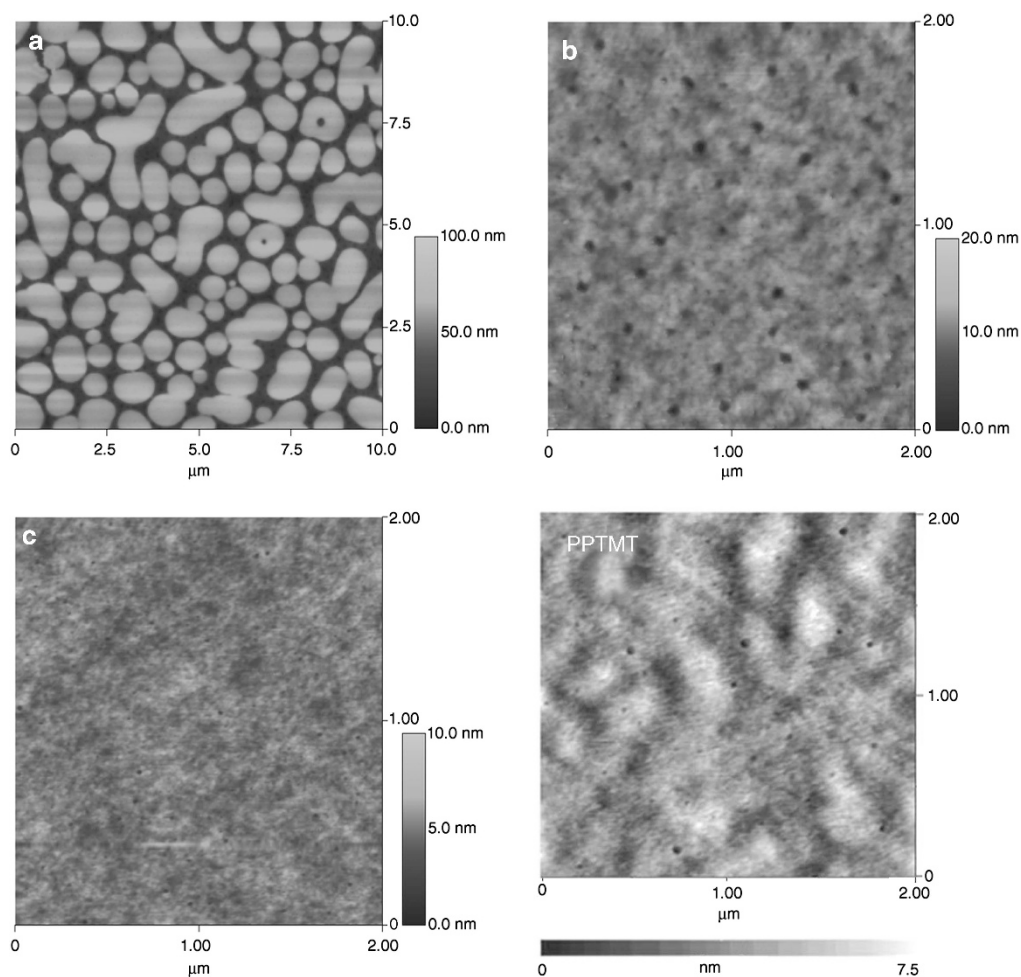


Figure 5 Topography image obtained using tapping-mode atomic force microscopy illustrating the morphology of the blend films spin-coated from chlorobenzene (a) P1/PC₇₁BM (w/w, 1:5); (b) P2/PC₇₁BM (w/w, 1:4); and (c) P3/PC₇₁BM (w/w, 1:4). PPTMT, poly(10-hexyl-10H-phenothiazine-3,7-ylene)-alt-2-(2,6-bis((E)-2-(5-bromo-3,4-dihexylthiophen-2-yl) vinyl)-4H-pyran-4-ylidene)malononitri). A full color version of this figure is available at *Polymer Journal* online.

the key elements in determining the PCE of polymer photovoltaic cells.⁴⁴ Figure 5 presents the atomic force microscopic height images of the three blend films with different weight ratios (1:5 w/w for P1, 1:4 w/w for P2 and P3, 1:3 w/w for PPTMT) for effective comparison and further elucidation of the difference in PSC performance. As clearly evidenced by the atomic force microscopic images, the P1:PC₇₁BM blend film has the coarsest surface, with a root-mean-square (rms) of 16.64 nm, and it exhibits clear PC₇₁BM grain-aggregation, with a size distribution of approximately 250 nm being almost homogeneously dispersed in the P1 matrix, which may result in large-scale phase separation, decreased diffusional escape probability for mobile charge carriers and, hence, increased recombination. This finding is fully consistent with the relatively low short circuit densities obtained for the P1:PC₇₁BM cell (1.55 mA cm⁻²). Compared with P1, the blend films of P2 and P3 have a flat surface, with rms values of approximately 1.30 and 0.54 nm, respectively, and the blend film of PPTMT has an rms value of approximately 1.17 nm with little aggregation. Because P2 and P3 have good miscibility with PC₇₁BM and an increased interfacial area between the polymer and PC₇₁BM is expected, the J_{sc} of the P2- and P3-based devices increases to 2.17 and 2.44 mA cm⁻², respectively.

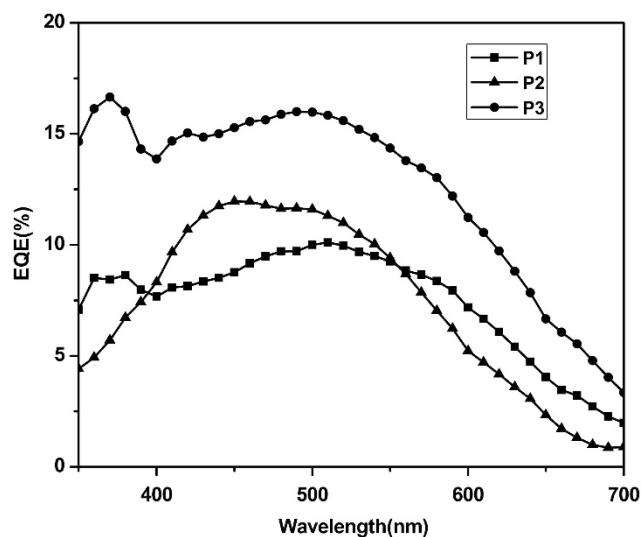


Figure 6 External quantum efficiencies (EQEs) of the polymer solar cells based on the blend of copolymers and PC₇₁BM.

Figure 6 presents the external quantum efficiency spectra of the devices based on P1:PC₇₁BM, P2:PC₇₁BM and P3:PC₇₁BM. The spectra demonstrate that the PSC devices have a good response to sunlight in the range from 350 to 700 nm. The device based on P3 exhibits the best external quantum efficiency to sunlight in the entire range, compared with the devices based on P1 and P2, due to the stronger and broader absorption of P3 (Figure 2).

CONCLUSIONS

Alternating copolymers containing electron-rich (carbazole, triphenylamine, phenothiazine) and electron-deficient (PM) units connected by a 2,5-divinylthiophene unit were synthesized via a Heck coupling reaction. Although the double bond was induced to link the donor unit and the acceptor unit, the polymers also exhibited high thermal stability up to 324, 346 and 341 °C. UV-vis absorption and cyclic voltammetric experiments demonstrated that the introduction of the double bond in the polymer main chain results in an enhancement of the conjugated length, extension of the absorption spectral range and decreased band gap of the polymers. In addition, BHJ PSCs were fabricated with the conjugated polymers as the electron donors and PC₇₁BM as the electron acceptor. The PCEs of the PSCs based on P1, P2, and P3 reached 0.36, 0.41 and 0.47%, respectively, under AM 1.5, 100 mW cm⁻² illumination.

ACKNOWLEDGEMENTS

This work was supported by the State Key Development Program for Basic Research of China (Grant 2009CB623605), the National Natural Science Foundation of China (Grant 20874035) and the Project of Jilin Province (Grant 20080305).

- Hoppe, H. & Sariciftci, N. S. Organic solar cells: an overview. *J. Mater. Res.* **19**, 1924–1945 (2004).
- Winder, C. & Sariciftci, N. S. Low bandgap polymers for photon harvesting in bulk heterojunction solar cells. *J. Mater. Chem.* **14**, 1077–1084 (2004).
- Gunes, H., Neugebauer, H. S. & Sariciftci, N. S. Conjugated polymer-based organic solar cells. *Chem. Rev.* **107**, 1324–1338 (2007).
- He, Y. J. & Li, Y. F. Fullerene derivative acceptor for high performance polymer solar cells. *Phys. Chem. Chem. Phys.* **13**, 1970–1983 (2010).
- Tamayo, A. B., Dang, X. D., Walker, B., Seo, J., Kent, T. & Nguyen, T. Q. A low band gap, solution processable oligothiophene with a dialkylated diketopyrrolopyrrole chromophore for use in bulk heterojunction solar cells. *Appl. Phys. Lett.* **94**, 103301–103303 (2009).
- Wen, S. P., Dong, Q. F., Cheng, W. D., Li, P. F., Xu, B. & Tian, W. J. A benzo[1,2-*b*:4,5-*b'*]dithiophene-based copolymer with deep HOMO level for efficient polymer solar cells. *Solar Energy Mater. Solar Cells* **100**, 239–245 (2012).
- Hou, J. H., Tan, Z. A., Yan, Y., He, Y. J., Yang, C. H. & Li, Y. F. Synthesis and photovoltaic properties of two-dimensional conjugated polythiophenes with bi(thiophenevinylene) side chains. *J. Am. Chem. Soc.* **128**, 4911–4916 (2006).
- Service, R. F. Outlook brightens for plastic solar cells. *Science* **332**, 293 (2011).
- Yu, G., Gao, J., Hummelen, J. C., Wudl, F. & Heeger, A. J. Polymer photovoltaic cells: enhanced efficiencies via a network of internal donor-acceptor heterojunctions. *Science* **270**, 1789–1791 (1995).
- Li, C., Liu, M. Y., Pschirer, N. G., Baumgarten, M. & Mullen, K. Polyphenylene-based materials for organic photovoltaics. *Chem. Rev.* **110**, 6817–6855 (2010).
- Li, Y. F. & Zou, Y. P. Conjugated polymer photovoltaic materials with broad absorption band and high charge carrier mobility. *Adv. Mater.* **20**, 2952–2958 (2008).
- Cheng, Y. J., Yang, S. H. & Hsu, C. S. Synthesis of conjugated polymers for organic solar cell applications. *Chem. Rev.* **109**, 5868–5923 (2009).
- Wen, S. P., Pei, J. N., Zhou, Y. H., Xue, L. L., Xu, B., Li, Y. W. & Tian, W. J. Synthesis and photovoltaic properties of poly(p-phenylenevinylene) derivatives containing oxadiazole. *J. Polym. Sci. A Polym. Chem.* **47**, 1003–1012 (2009).
- Scharber, M. C., Muhlbacher, D., Koppe, M., Denk, P., Waldauf, C., Heeger, A. J. & Brabec, C. L. Design rules for donors in bulk-heterojunction solar cells—towards 10% energy-conversion efficiency. *Adv. Mater.* **18**, 789–794 (2006).
- He, Y. J., Chen, H. Y., Hou, J. H. & Li, Y. F. Indene-C₆₀ bisadduct: a new acceptor for high-performance polymer solar cells. *J. Am. Chem. Soc.* **132**, 1377–1382 (2010).
- Zhao, G. J., He, Y. J. & Li, Y. F. 6.5% efficiency of polymer solar cells based on poly(3-hexylthiophene) and indene-C₆₀ bisadduct by device optimization. *Adv. Mater.* **22**, 4355–4358 (2010).
- Zhou, E. J., Hou, J. H., Yang, C. H. & Li, Y. F. Synthesis and properties of polythiophenes with conjugated side-chains containing carbon-carbon double and triple bonds. *J. Polym. Sci. A Polym. Chem.* **44**, 2206–2214 (2006).
- Chu, T. Y., Lu, J. P., Beaupre, S., Zhang, Y. G., Pouliot, J. R., Wakim, S., Zhou, J. Y., Leclerc, M., Li, Z., Ding, J. F. & Tao, Y. Bulk heterojunction solar cells using thieno[3,4-*c*]pyrrole-4,6-dione and dithieno[3,2-*b*:2',3'-*d'*]silole copolymer with a power conversion efficiency of 7.3%. *J. Am. Chem. Soc.* **133**, 4250–4253 (2011).
- Zhou, E. J., Cong, J. Z., Tajima, K. & Hashimoto, K. Synthesis and photovoltaic properties of donor-acceptor copolymers based on 5,8-dithien-2-yl-2,3-diphenylquinoxaline. *Chem. Mater.* **22**, 4890–4895 (2010).
- Wen, S. P., Pei, J. N., Li, P. F., Zhou, Y. H., Cheng, W. D., Dong, Q. F., Li, Z. F. & Tian, W. J. Synthesis and photovoltaic properties of low-bandgap 4,7-dithien-2-yl-2,1,3-benzothiadiazole-based poly(heteroarylenevinylene)s. *J. Polym. Sci. A Polym. Chem.* **49**, 2715–2724 (2011).
- Li, Q., Liu, L. J., Liu, Z. Y., Li, Z. F., Cheng, W. D., Wen, S. P., Li, P. F., Li, Z. J. & Tian, W. J. Synthesis and photovoltaic property of a novel low band gap conjugated donor-acceptor copolymer consisting of 2,7-carbazole and (bithiophenevinyl)-(2-pyran-4-ylidene)malononitrile (TVM). *Synthetic Metals* **161**, 731–736 (2011).
- Lu, J. P., Liang, J., Drolet, N., Ding, J., Tao, Y. & Movileanu, R. Crystalline low band-gap alternating indolocarbazole and benzothiadiazole-cored oligothiophene copolymer for organic solar cell applications. *Chem. Commun.* **42**, 5315–5317 (2008).
- Zhu, Z. G., Waller, D., Gaudiana, R., Morana, M., Muhlbacher, D., Scharber, M. C. & Brabec, C. Panchromatic conjugated polymers containing alternating donor/acceptor units for photovoltaic applications. *Macromolecules* **40**, 1981–1896 (2007).
- Hou, J. H., Chen, H. Y., Zhang, S. Q., Li, G. & Yang, Y. Synthesis, characterization, and photovoltaic properties of a low band gap polymer based on silole-containing polythiophenes and 2,1,3-benzothiadiazole. *J. Am. Chem. Soc.* **130**, 16144–16145 (2008).
- Pan, H. L., Li, Y. N., Wu, Y. L., Liu, P., Ong, B. S., Zhu, S. P. & Xu, G. Synthesis and thin-film transistor performance of poly(4,8-didodecylbenzo[1,2-*b*:4,5-*b'*]dithiophene). *Chem. Mater.* **18**, 3237–3241 (2006).
- Wen, S. P., Pei, J. N., Zhou, Y. H., Li, P. F., Xue, L. L., Li, Y. W., Xu, B. & Tian, W. J. Synthesis of 4,7-diphenyl-2,1,3-benzothiadiazole-based copolymers and their photovoltaic applications. *Macromolecules* **42**, 4977–4984 (2009).
- Wienk, M., Turbiez, M., Gilot, J. & Janssen, R. A. J. Narrow-bandgap diketopyrrolopyrrole polymer solar cells: the effect of processing on the performance. *Adv. Mater.* **20**, 2556–2560 (2008).
- Liang, Y. Y., Xu, Z., Xia, J. B., Tsai, S., Wu, Y., Li, G., Ray, C. & Yu, L. P. For the bright future—bulk heterojunction polymer solar cells with power conversion efficiency of 7.4%. *Adv. Mater.* **22**, E135–E138 (2010).
- Zou, Y. P., Najari, A., Berrouard, P., Beaupre, S., Aich, B. R., Tao, Y. & Leclerc, M. A thieno[3,4-*c*]pyrrole-4,6-dione-based copolymer for efficient solar cells. *J. Am. Chem. Soc.* **132**, 5330–5331 (2010).
- Li, Y. W., Xue, L. L., Li, H., Li, Z. F., Xu, B., Wen, S. P. & Tian, W. J. Energy level and molecular structure engineering of conjugated donor-acceptor copolymers for photovoltaic applications. *Macromolecules* **42**, 4491–4499 (2009).
- Chan, S. H., Chen, C. P., Chao, T. C., Ting, C., Lin, C. S. & Ko, C. S. Synthesis, characterization, and photovoltaic properties of novel semiconducting polymers with thiophene-phenylene-thiophene (TPT) as coplanar units. *Macromolecules* **41**, 5519–5526 (2008).
- Anuragudom, P., Newaz, S. S., Phanichphant, S. & Lee, T. R. Synthesis of defect-free poly(9,9-dialkylfluorenyl-2,7-vinylene). *Macromolecules* **39**, 3494–3499 (2006).
- Kong, X., Kulkarni, A. P. & Jenekhe, S. A. Phenothiazine-based conjugated polymers: synthesis, electrochemistry, and light-emitting properties. *Macromolecules* **36**, 8992–8999 (2003).
- Woods, L. L. Some further reactions of 2,6-dimethyl-4-pyrone. *J. Am. Chem. Soc.* **80**, 1440–1442 (1958).
- Kagan, J. & Arora, S. K. Synthesis of alpha-thiophene oligomers via 1,3-butadiynes. *J. Org. Chem.* **48**, 4317–4320 (1983).
- Pei, J. N., Wen, S. P., Zhou, Y. H., Dong, Q. F., Liu, Z. Y., Zhang, J. B. & Tian, W. J. A low band gap donor-acceptor copolymer containing fluorene and benzothiadiazole units: synthesis and photovoltaic properties. *N. J. Chem.* **35**, 385–393 (2011).
- Peng, Q., Park, K., Lin, T., Durstock, M. & Dai, L. M. Donor-π-acceptor conjugated copolymers for photovoltaic applications: tuning the open-circuit voltage by adjusting the donor/acceptor ratio. *J. Phys. Chem. B.* **112**, 2801–2808 (2008).
- Yamamoto, T., Komarudin, D., Arai, M., Lee, B. L., Suganuma, H., Asakawa, N., Inoue, Y., Kubota, K., Sasaki, S., Fukuda, T. & Matsuda, H. Extensive studies on π-stacking of poly(3-alkylthiophene-2,5-diyl)s and poly(4-alkylthiazole-2,5-diyl)s by optical spectroscopy, NMR analysis, light scattering analysis, and X-ray crystallography. *J. Am. Chem. Soc.* **120**, 2047–2058 (1998).
- Pommerehne, J., Vestweber, H., Guss, W., Maht, R. F., Bassler, H., Porsch, M. & Daub, J. Efficient two layer leds on a polymer blend basis. *Adv. Mater.* **7**, 551–554 (1995).
- Shi, C. J., Yao, Y., Yang, Y. & Pei, Q. B. Regioregular copolymers of 3-alkoxythiophene and their photovoltaic application. *J. Am. Chem. Soc.* **128**, 8980–8986 (2006).
- Shaheen, S. E., Brabec, C. J. & Sariciftci, N. S. 2.5% efficient organic plastic solar cells. *Appl. Phys. Lett.* **78**, 841–843 (2001).
- Mihailtchi, V. D., Blorn, P. W. M., Hummelen, J. C. & Rispens, M. T. Cathode dependence of the open-circuit voltage of polymer:fullerene bulk heterojunction solar cells. *J. Appl. Phys.* **94**, 6849–6854 (2003).
- Dyakonov, V. Mechanisms controlling the efficiency of polymer solar cells. *Appl. Phys.* **A**, 79, 21–25 (2004).
- Hoppe, H. N. & Sariciftci, S. Morphology of polymer/fullerene bulk heterojunction solar cells. *J. Mater. Chem.* **16**, 45–61 (2006).